

# An Incremental SVD Method for Non-Fickian Flows in Porous Media: Addressing Storage and Computational Challenges

Gang Chen\*

Yangwen Zhang<sup>†</sup>

Dujin Zuo \*

August 30, 2023

## Abstract

It is well known that the numerical solution of the Non-Fickian flows at the current stage depends on all previous time instances. Consequently, the storage requirement increases linearly, while the computational complexity grows quadratically with the number of time steps. This presents a significant challenge for numerical simulations, and to the best of our knowledge, it remains an unresolved issue. In this paper, we present a memory-free algorithm, based on the incremental SVD technique, that exhibits only linear growth in computational complexity as the number of time steps increases. We prove that the error between the solutions generated by the conventional algorithm and our innovative approach lies within the scope of machine error. Numerical experiments are showcased to affirm the accuracy and efficiency gains in terms of both memory usage and computational expenses.

## 1 Introduction

The non-Fickian flow of fluid in porous media [6] is complicated by the history effect which characterizes various mixing length growth of the flow and can be modeled by an integro-differential equation: Find  $u = u(x, t)$  such that

$$u_t + \mathcal{A}u + \int_0^t K(t-s)\mathcal{B}u(s)ds = f(x, t), \quad \text{in } \Omega \times (0, T], \quad (1.1a)$$

$$u = 0, \quad \text{on } \partial\Omega \times (0, T], \quad (1.1b)$$

$$u(x, 0) = u_0(x), \quad \text{in } \Omega, \quad (1.1c)$$

where  $\Omega \in \mathbb{R}^d (d = 1, 2, 3)$  is a bounded convex polygonal domain with Lipschitz boundary  $\partial\Omega$ ,  $u_0$  is a given function defined on  $\Omega$ ,  $K(t)$  is a nonnegative memory kernel,  $f(x, t)$  is a known function,  $\mathcal{A}$  is a symmetric positive definite second-order elliptic operator and is of the form:

$$\mathcal{A} = - \sum_{i,j=1}^d \frac{\partial}{\partial x_i} (a_{ij}(x) \frac{\partial}{\partial x_j}) + a(x)I, \quad a(x) \geq 0,$$

$$a_{ij}(x) = a_{ji}(x), \quad i, j = 1, \dots, d, \quad a_1 \sum_{i=1}^d \xi_i^2 \geq \sum_{i,j=1}^d a_{ij} \xi_i \xi_j \geq a_0 \sum_{i=1}^d \xi_i^2, \quad a_1 \geq a_0 > 0.$$

\*College of Mathematics, Sichuan University, Chengdu 610064, China (cglwdm@uestc.edu.cn, zuodujin@stu.scu.edu.cn).

<sup>†</sup>Department of Mathematics, University of Louisiana at Lafayette, Lafayette, LA 70503, USA (yangwen.zhang@louisiana.edu).

The operator  $\mathcal{B}$  is any second-order linear operator and takes the following form:

$$\mathcal{B} = - \sum_{i,j=1}^d \frac{\partial}{\partial x_i} (b_{ij}(x) \frac{\partial}{\partial x_j}) + \sum_{i=1}^d b_i(x) \frac{\partial}{\partial x_i} + b(x)I.$$

Numerous numerical approaches have been put forth to address the problem (1.1). Among the array of computational techniques available, finite difference for time discretization and Galerkin finite element for spatial discretization have gained significant prominence. Time discretization methods encompass strategies rooted in backward Euler, Crank-Nicolson, as well as their hybrid variants. As for spatial discretization, a range of methodologies are employed, including conventional finite element methods [1, 3, 16, 17, 19, 21, 29], mixed finite element methods [6, 13, 14, 26], finite volume method [25] and discontinuous Galerkin methods [22]. For further information, refer to [2, 9, 15, 20, 27, 28] and the citations therein.

One challenge faced by these numerical schemes is the need to store all preceding time numerical solutions when computing the solution at the next step. The storage requirement increases linearly while the computational complexity grows quadratically with the number of time steps, see more details in Section 2. This poses a substantial challenge for numerical simulations. To address this issue, we adopt the incremental singular value decomposition (SVD) algorithm to compress the data while simultaneously solving the equation (1.1).

The incremental SVD, initially introduced by Brand [4], provides an efficient approach to compute the SVD of a matrix. This method begins by initializing the incremental SVD using a small dataset, subsequently updating it as new data becomes accessible. This technique finds diverse applications, encompassing tasks such as recommender systems [10], proper orthogonal decomposition [7, 8], dynamic mode decomposition [12] and visual tracking [23]. The algorithm necessitates the computation of thousands or even millions of orthogonal matrices, which are subsequently multiplied together. Nonetheless, these multiplications have the potential to destroy the orthogonality. Consequently, many reorthogonalizations are imperative in practical implementation. Brand addressed this matter in [5], noting, “It is an open question how often this is necessary to guarantee a certain overall level of numerical precision; it does not change the overall complexity.” A subsequent work [30] provided a response to this query, suggesting a method to mitigate the need for extensive orthogonal matrix computations and thereby eliminating the necessity for reorthogonalizations. Moreover, they demonstrated that this modification does not adversely impact the algorithm’s outcomes.

Our approach is to simultaneously solve the integro-differential equation (1.1) and compress the solution data using the incremental SVD method. The incremental SVD algorithm can be easily used in conjunction with a time stepping code for simulating equation (1.1). This approach enables storing solution data in several smaller matrices, alleviating the need for a huge dense matrix as often seen in traditional methods. As a result, we are able to address the issue of data storage in solving the integro-differential equation (1.1).

The subsequent sections of this paper are thoughtfully structured as follows. In Section 2, we provide an overview of the standard finite element method employed for spatial discretization, coupled with the back Euler method utilized for time discretization in order to tackle the integro-differential equation (1.1). We demonstrate that the storage requirement increases linearly, while the computational complexity grows quadratically with the number of time steps  $n$  in this standard approach. Moving on to Section 3, we delve into a review of the improved incremental SVD algorithm introduced in [30]. Within Section 4, we present a novel algorithm for resolving the integro-differential equation (1.1), leveraging the improved incremental SVD approach. We establish that our novel algorithm maintains memory efficiency under the premise of low-rank data,

and it demonstrates exclusively linear growth in computational complexity with the progression of time steps. In Section 5, we present a rigorous error analysis for our approach, demonstrating that the convergence rates are equivalent to traditional methods. The numerical experiments in Section 6 further confirm the efficiency of our new algorithm in terms of both memory usage and computational performance. Finally, we discuss potential future work in the conclusion.

## 2 The finite element method for integro-differential equations

In this section, our objective is to present the finite element method for integro-differential equations.

Let  $\mathcal{T}_h$  represent a collection of regular simplices  $K$  that partition the domain  $\Omega$ , and  $\mathcal{P}_k(K)$  ( $k \geq 1$ ) denote the polynomial space defined on the element  $K$  with a maximum degree of  $k$ . Utilizing the triangulation  $\mathcal{T}_h$ , we can define the continuous piecewise finite element space  $V_h$  as follows:

$$V_h = \{v_h \in H_0^1(\Omega) : v_h|_K \in \mathcal{P}_k(K), \forall K \in \mathcal{T}_h\}.$$

The semidiscrete Galerkin scheme for the integro-differential equation (1.1) can be expressed as follows: seek  $u_h(t) \in V_h$  such that

$$(u_{h,t}, v_h) + \mathcal{A}(u_h, v_h) + \int_0^t K(t-s) \mathcal{B}(u_h(s), v_h) ds = (f, v_h), \quad \forall v_h \in V_h, \quad (2.1a)$$

$$u_h(0) = u_h^0 \in V_h, \quad (2.1b)$$

where  $u_h^0$  corresponds to the projection of  $u_0$  onto the space  $V_h$ ,  $u_{h,t}$  denotes the time derivative of  $u_h$ , while  $\mathcal{A}(\cdot, \cdot)$ ,  $\mathcal{B}(\cdot, \cdot)$  represent the bilinear forms associated with the operator  $\mathcal{A}$  and  $\mathcal{B}$ , defined on  $H_0^1(\Omega) \times H_0^1(\Omega)$ , and takes the following forms:

$$\begin{aligned} \mathcal{A}(u, v) &= \sum_{i,j=1}^d \left( a_{ij}(x) \frac{\partial u}{\partial x_i}, \frac{\partial v}{\partial x_j} \right) + (a(x)u, v), \\ \mathcal{B}(u, v) &= \sum_{i,j=1}^d \left( b_{ij}(x) \frac{\partial u}{\partial x_i}, \frac{\partial v}{\partial x_j} \right) + \sum_{i=1}^d (b_i(x) \frac{\partial u}{\partial x_i}, v) + (b(x)u, v). \end{aligned}$$

Here,  $(\cdot, \cdot)$  represents the inner product in  $L^2(\Omega)$ .

In the discretization of the time domain, we employ the backward Euler method. To achieve this, we select a time step size  $\Delta t$  and uniformly partition the time domain  $[0, T]$  into  $n$  steps, where  $T = n\Delta t$ . We denote  $t_i = i\Delta t$  and utilize numerical quadrature as follows:

$$\sum_{j=0}^i \omega_{i+1,j} g(t_j) \approx \int_0^{t_{i+1}} K(t_{i+1}-s) g(s) ds,$$

where  $\omega_{i+1,j} = \Delta t \cdot K(t_{i+1}-t_j)$  for  $j = 0, 1, \dots, i$ .

Then, the fully discrete scheme is expressed as follows: given  $u_h^0 \in V_h$ , we aim to find  $u_h^{i+1} \in V_h$  for all  $i = 0, 1, \dots, n-1$ , satisfying

$$\left( \frac{u_h^{i+1} - u_h^i}{\Delta t}, v_h \right) + \mathcal{A}(u_h^{i+1}, v_h) + \sum_{j=0}^i \omega_{i+1,j} \mathcal{B}(u_h^j, v_h) = (f^{i+1}, v_h), \quad \forall v_h \in V_h, \quad (2.2)$$

which is equivalent to

$$(u_h^{i+1}, v_h) + \Delta t \mathcal{A}(u_h^{i+1}, v_h) = (u_h^i, v_h) - \Delta t \sum_{j=0}^i \omega_{i+1,j} \mathcal{B}(u_h^j, v_h) + \Delta t (f^{i+1}, v_h), \quad (2.3)$$

for all  $v_h \in V_h$  and  $f^{i+1}$  denotes the value of the function  $f$  at time  $t_{i+1}$ .

Next, we assume that  $V_h = \text{span}\{\phi_1, \dots, \phi_m\}$ , and we define the matrices  $M$ ,  $A$ ,  $B$  and vector  $b_{i+1}$  as follows:

$$\begin{aligned} M_{ij} &= (\phi_i, \phi_j), \quad A_{ij} = \sum_{k,\ell=1}^d \left( a_{k\ell}(x) \frac{\partial \phi_i}{\partial x_k}, \frac{\partial \phi_j}{\partial x_\ell} \right) + (a(x) \phi_i, \phi_j), \quad (b_{i+1})_j = (f^{i+1}, \phi_j), \\ B_{ij} &= \sum_{k,\ell=1}^d \left( b_{k\ell}(x) \frac{\partial \phi_i}{\partial x_k}, \frac{\partial \phi_j}{\partial x_\ell} \right) + \sum_{k=1}^d (b_k(x) \frac{\partial \phi_i}{\partial x_k}, \phi_j) + (b(x) \phi_i, \phi_j), \end{aligned} \quad (2.4)$$

where  $X_{ij}$  represents the element of row  $i$  and column  $j$  of matrix  $X$ , and  $(\alpha)_j$  denotes the  $j$ -th component of the vector  $\alpha$ . Let  $u_{i+1}$  be the coefficients of  $u_h^{i+1}$  at time  $t_{i+1}$ , given by:

$$u_h^{i+1} = \sum_{j=1}^m (u_{i+1})_j \phi_j. \quad (2.5)$$

Substituting (2.4) and (2.5) into (2.3), we obtain the following algebraic system:

$$(M + \Delta t A) u_{i+1} = M u_i - \Delta t B \sum_{j=0}^i \omega_{i+1,j} u_j + \Delta t b_{i+1}. \quad (2.6)$$

By solving the above algebraic system, we can obtain the solution to (2.3). The algorithm is presented in Algorithm 1.

---

**Algorithm 1** (Finite element and backward Euler method for solving equation (1.1))

---

**Require:**  $\Delta t$ ,  $M \in \mathbb{R}^{m \times m}$ ,  $A \in \mathbb{R}^{m \times m}$ ,  $B \in \mathbb{R}^{m \times m}$ ,  $u_0$

- 1: Set  $\tilde{A} = M + \Delta t A$ ,  $U = \mathbf{zeros}(m, n+1)$ ,  $U(:, 1) = u_0$
- 2: **for**  $i = 0$  to  $n-1$  **do**
- 3:   Compute the weights  $\omega_{i+1,j}$  ( $j = 0, 1, \dots, i$ ) and get the load vector  $b_{i+1}$
- 4:    $\tilde{b}_{i+1} = M U(:, i+1) - \Delta t B \sum_{j=0}^i \omega_{i+1,j} U(:, j+1) + \Delta t b_{i+1}$
- 5:   Solve  $\tilde{A} u_{i+1} = \tilde{b}_{i+1}$
- 6:    $U(:, i+2) = u_{i+1}$
- 7: **end for**

**Ensure:**  $u_n$

---

However, it becomes evident that solving the algebraic system (2.6) poses a significant computational challenge. To compute the numerical solution  $u_h^{i+1}$ , all the preceding time numerical solutions  $\{u_h^j\}_{j=0}^i$  must be available. As the coefficients  $\{\omega_{i+1,j}\}_{j=0}^i$  change with each time step  $i$ , it becomes necessary to store all the numerical solutions  $\{u_h^j\}_{j=0}^i$ . The storage cost of the history term is

$$\mathcal{O}(mn), \quad (2.7)$$

and the computational cost is:

$$\sum_{i=1}^n \sum_{j=0}^i \mathcal{O}(m) = \mathcal{O}(mn^2). \quad (2.8)$$

Consequently, the storage requirement increases linearly while the computational complexity grows quadratically with the number of time steps  $n$ . This poses a substantial challenge for numerical simulations.

Fortunately, the memory and computational complexity issue mentioned above can be addressed with the help of the incremental singular value decomposition (SVD) method, provided we make the assumption that the solution data exhibits approximate low rank.

### 3 The incremental SVD method

We begin by introducing several crucial definitions and concepts that are essential for understanding the incremental SVD method. Given a vector  $u \in \mathbb{R}^m$  and an integer  $r$  satisfying  $r \leq m$ , the notation  $u(1:r)$  denotes the first  $r$  components of  $u$ . Likewise, for a matrix  $U \in \mathbb{R}^{m \times n}$ , we use the notation  $U(p:q, r:s)$  to refer to the submatrix of  $U$  that encompasses the entries from rows  $p$  to  $q$  and columns  $r$  to  $s$ .

Throughout this section, we make the assumption that the rank of the matrix  $U \in \mathbb{R}^{m \times n}$  is low, specifically denoted by  $\text{rank}(U) \ll \min\{m, n\}$ .

Next, we present an improved version of Brand's incremental SVD algorithm from [30]. The algorithm updates the SVD of a matrix when one or more columns are added to the matrix. We split the process into four steps.

#### Step 1: Initialization

Assuming that the first column of matrix  $U$ , denoted as  $u_1$ , is non-zero, we can proceed to initialize the SVD of  $u_1$  using the following approach:

$$\Sigma = (u_1^\top u_1)^{1/2}, \quad Q = u_1 \Sigma^{-1}, \quad R = 1.$$

The algorithm is shown in Algorithm 2.

---

#### Algorithm 2 (Initialize ISVD)

---

**Require:**  $u_1 \in \mathbb{R}^m$

1:  $\Sigma = (u_1^\top u_1)^{1/2}; \quad Q = u_1 \Sigma^{-1}; \quad R = 1$

**Ensure:**  $Q, \Sigma, R$

---

Assuming we already have the truncated SVD of rank  $k$  for the first  $\ell$  columns of matrix  $U$ , denoted as  $U_\ell$ :

$$U_\ell \approx Q \Sigma R^\top, \quad \text{with} \quad Q^\top Q = I_k, \quad R^\top R = I_k, \quad \Sigma = \text{diag}(\sigma_1, \dots, \sigma_k), \quad (3.1)$$

where  $\Sigma \in \mathbb{R}^{k \times k}$  is a diagonal matrix with the  $k$  ordered singular values of  $U_\ell$  on the diagonal,  $Q \in \mathbb{R}^{m \times k}$  is the matrix of the corresponding  $k$  left singular vectors of  $U_\ell$  and  $R \in \mathbb{R}^{\ell \times k}$  is the matrix of the corresponding  $k$  right singular vectors of  $U_\ell$ .

Given our assumption that the matrix  $U$  is low rank, it is reasonable to expect that most of the columns of  $U$  are either linearly dependent or nearly linearly dependent on the vectors in  $Q \in \mathbb{R}^{m \times k}$ .

Without loss of generality, we assume that the next  $s$  vectors, denoted as  $\{u_{\ell+1}, \dots, u_{\ell+s}\}$ , their residuals are less than a specified tolerance when projected onto the subspace spanned by the columns of  $Q$ . However, the residual of  $u_{\ell+s+1}$  is larger than the given tolerance. In other words,

$$|u_i - QQ^\top u_i| < \text{tol}, \quad i = \ell + 1, \dots, \ell + s, \quad (3.2a)$$

$$|u_i - QQ^\top u_i| \geq \text{tol}, \quad i = \ell + s + 1. \quad (3.2b)$$

### Step 2: Update the SVD of $U_{\ell+s}$ ( $p$ -truncation)

By the assumption (3.2a), we have

$$\begin{aligned} U_{\ell+s} &= [U_\ell \mid u_{\ell+1} \mid \dots \mid u_{\ell+s}] \\ &\approx [Q\Sigma R^\top \mid u_{\ell+1} \mid \dots \mid u_{\ell+s}] \\ &\approx [Q\Sigma R^\top \mid QQ^\top u_{\ell+1} \mid \dots \mid QQ^\top u_{\ell+s}] \\ &= Q \underbrace{\left[ \Sigma \mid Q^\top u_{\ell+1} \mid \dots \mid Q^\top u_{\ell+s} \right]}_Y \begin{bmatrix} R & 0 \\ 0 & I_s \end{bmatrix}^\top. \end{aligned}$$

We can obtain the truncated SVD of  $U_{\ell+s}$  by computing the full SVD of the matrix  $Y$ . Specifically, let  $Y = Q_Y \Sigma_Y R_Y^\top$  be the SVD of  $Y$ , and split  $R_Y$  into  $\begin{bmatrix} R_Y^{(1)} \\ R_Y^{(2)} \end{bmatrix}$ . With this, we can update the SVD of  $U_{\ell+s}$  as follows:

$$Q \leftarrow QQ_Y, \quad \Sigma \leftarrow \Sigma_Y, \quad R \leftarrow \begin{bmatrix} RR_Y^{(1)} \\ R_Y^{(2)} \end{bmatrix} \in \mathbb{R}^{(\ell+s) \times \ell}.$$

It is worth noting that the dimension of the matrices  $Q$  and  $\Sigma$  remains unchanged, and we need to incrementally store the matrix  $W = [Q^\top u_{\ell+1} \mid \dots \mid Q^\top u_{\ell+s}]$ . As  $W$  belongs to  $\mathbb{R}^{k \times s}$  where  $k \leq r$  is relatively small, the storage cost for this matrix is low.

### Step 3: Update the SVD of $U_{\ell+s+1}$ (No truncation)

Next, we proceed with the update of the SVD for  $U_{\ell+s+1}$ . Firstly, we compute the residual vector of  $u_{\ell+s+1}$  by projecting it onto the subspace spanned by the columns of  $Q$ , i.e.,

$$e = u_{\ell+s+1} - QQ^\top u_{\ell+s+1}. \quad (3.3)$$

First, we define  $p = \|e\|$ . Then, based on (3.2b), we deduce that  $p > \text{tol}$ . Finally, we denote  $\tilde{e}$  as  $e/p$ . With these definitions, we establish the following fundamental identity:

$$\begin{aligned} U_{\ell+s+1} &= [U_{\ell+s} \mid u_{\ell+s+1}] \\ &\approx [Q\Sigma R^\top \mid p\tilde{e} + QQ^\top u_{\ell+s+1}] \\ &\approx [Q \mid \tilde{e}] \underbrace{\begin{bmatrix} \Sigma & Q^\top u_{\ell+s+1} \\ 0 & p \end{bmatrix}}_{\tilde{Y}} \begin{bmatrix} R & 0 \\ 0 & 1 \end{bmatrix}^\top, \end{aligned}$$

Let  $\bar{Q}\bar{\Sigma}\bar{R}^\top$  be the full SVD of  $\bar{Y}$ . Then the SVD of  $U_{\ell+s+1}$  can be approximated by

$$U_{\ell+s+1} \approx ([Q \mid \tilde{e}]\bar{Q})\bar{\Sigma} \left( \begin{bmatrix} R & 0 \\ 0 & 1 \end{bmatrix} \bar{R} \right)^\top.$$

With this, we can update the SVD of  $U_{\ell+s+1}$  as follows:

$$Q \leftarrow ([Q \mid \tilde{e}])\bar{Q}, \quad \Sigma \leftarrow \bar{\Sigma}, \quad R \leftarrow \begin{bmatrix} R & 0 \\ 0 & 1 \end{bmatrix} \bar{R}.$$

It is worth noting that, in this case, the dimensions of the matrices  $Q$  and  $\Sigma$  increase.

**Remark 1.** Theoretically, the residual vector  $e$  in (3.3) is orthogonal to the vectors in the subspace spanned by the columns of  $Q$ . However, in practice, this orthogonality can be completely lost, a fact that has been confirmed by numerous numerical experiments [7,8,18]. In [11], Giraud et al. stressed that exactly two iteration-steps are enough to keep the orthogonality. To reduce computational costs, Zhang [30] suggested using the two iteration steps only when the inner product between  $e$  and the first column of  $Q$  exceeds a certain tolerance. Drawing from our experience, it is imperative to calibrate this tolerance to align closely with the machine error. For instance, as demonstrated in this paper, we consistently establish this tolerance as  $10^{-14}$ .

#### Step 4: Singular value truncation

For many PDE data sets, they may have a large number of nonzero singular values but most of them are very small. Considering the computational cost involved in retaining all of these singular values, it becomes necessary to perform singular value truncation. This involves discarding the last few singular values if they fall below a certain tolerance threshold.

**Lemma 1.** [30, Lemma 5.1] Assume that  $\Sigma = \text{diag}(\sigma_1, \sigma_2, \dots, \sigma_k)$  with  $\sigma_1 \geq \sigma_2 \geq \dots \geq \sigma_k$ , and  $\bar{\Sigma} = \text{diag}(\mu_1, \mu_2, \dots, \mu_{k+1})$  with  $\mu_1 \geq \mu_2 \geq \dots \geq \mu_{k+1}$ . Then we have

$$\mu_{k+1} \leq p, \tag{3.4}$$

$$\mu_{k+1} \leq \sigma_k \leq \mu_k \leq \sigma_{k-1} \leq \dots \leq \sigma_1 \leq \mu_1. \tag{3.5}$$

The inequality (3.4) indicates that, regardless of the magnitude of  $p$ , the last singular value of  $\bar{Y}$  can potentially be very small. This implies that the tolerance set for  $p$  cannot prevent the algorithm from computing exceedingly small singular values. Consequently, an additional truncation is necessary when the data contains numerous very small singular values. Fortunately, inequality (3.5) assures us that only the last singular value of  $\bar{Y}$  has the possibility of being less than the tolerance. Therefore, it suffices to examine only the last singular value.

(i) If  $\Sigma_Y(k+1, k+1) \geq \text{tol}$ , then

$$Q \leftarrow [Q \mid \tilde{e}]Q_Y, \quad \Sigma \leftarrow \Sigma_Y, \quad R \leftarrow \begin{bmatrix} R & 0 \\ 0 & 1 \end{bmatrix} R_Y.$$

(ii) If  $\Sigma_Y(k+1, k+1) < \text{tol}$ , then

$$Q \leftarrow [Q \mid \tilde{e}]Q_Y(:, 1:k), \quad \Sigma \leftarrow \Sigma_Y(1:k, 1:k), \quad R \leftarrow \begin{bmatrix} R & 0 \\ 0 & 1 \end{bmatrix} R_Y(:, 1:k).$$

It is essential to note that  $p$ -truncation and no-truncation do not alter the previous data, whereas singular value truncation may potentially change the entire previous data. However, we can establish the following bound:

**Lemma 2.** Suppose  $Q\Sigma R^\top$  is the SVD of  $A \in \mathbb{R}^{m \times n}$ , where  $\{\sigma_i\}_{i=1}^r$  are the positive singular values. Let  $B = Q(:, 1:r-1)\Sigma(1:r-1, 1:r-1)(R(:, 1:r-1))^\top$ . We have:

$$\max\{|a_1 - b_1|, |a_2 - b_2|, \dots, |a_n - b_n|\} \leq \sigma_r.$$

Here,  $a_i$  and  $b_i$  correspond to the  $i$ -th columns present in matrices  $A$  and  $B$  respectively. The symbol  $|\cdot|$  denotes the Euclidean norm within the realm of  $\mathbb{R}^m$ .

The proof of Lemma 2 is straightforward, and thus we omit it here. Moving forward, we will provide a summary of the aforementioned four steps in Algorithm 3.

---

**Algorithm 3** (Update ISVD)

---

**Require:**  $Q \in \mathbb{R}^{m \times k}, \Sigma \in \mathbb{R}^{k \times k}, R \in \mathbb{R}^{\ell \times k}, \text{tol}, W, Q_0, q, u_{\ell+1}$ ,  
1: Set  $d = Q^\top u_{\ell+1}; e = u_{\ell+1} - Qd; p = (e^\top e)^{1/2}$ ;  
2: **if**  $p \geq \text{tol}$  **then**  
3:   **if**  $q > 0$  **then**  
4:     Set  $Y = [\Sigma \mid \text{cell2mat}(W)]; [Q_Y, \Sigma_Y, R_Y] = \text{svd}(Y, 'econ')$ ;  
5:     Set  $Q_0 = Q_0 Q_Y, \Sigma = \Sigma_Y, R_1 = R_Y(1:k, :), R_2 = R_Y(k+1:\text{end}, :), R = \begin{bmatrix} R R_1 \\ R_2 \end{bmatrix}; d = Q_Y^\top d$ ;  
6:   **end if**  
7:   Set  $Y = \begin{bmatrix} \Sigma & d \\ 0 & p \end{bmatrix}; [Q_Y, \Sigma_Y, R_Y] = \text{svd}(Y); e = e/p$ ;  
8:   **if**  $|e^\top Q(:, 1)| > 10^{-14}$  **then**  
9:      $e = e - Q(Q^\top e); p_1 = (e^\top e)^{1/2}; e = e/p_1$ ;  
10:   **end if**  
11:   Set  $Q_0 = \begin{bmatrix} Q_0 & 0 \\ 0 & 1 \end{bmatrix} Q_Y$ ;  
12:   **if**  $\Sigma_Y(k+1, k+1) \geq \text{tol}$  **then**  
13:      $Q = [Q \mid e]Q_0, \quad \Sigma = \Sigma_Y, \quad R = \begin{bmatrix} R & 0 \\ 0 & 1 \end{bmatrix} R_Y, \quad Q_0 = I_{k+1}$ ;  
14:   **else**  
15:      $Q = [Q \mid e]Q_0(:, 1:k), \Sigma = \Sigma_Y(1:k, 1:k), R = \begin{bmatrix} R & 0 \\ 0 & 1 \end{bmatrix} R_Y(:, 1:k), \quad Q_0 = I_k$ ;  
16:   **end if**  
17:    $W = []; q = 0$   
18: **else**  
19:    $q = q + 1; W\{q\} = d$ ;  
20: **end if**  
**Ensure:**  $Q, \Sigma, R, W, Q_0, q$

---

**Remark 2.** The set  $W$ , which is one of the outputs of Algorithm 3, has the potential to be non-empty. Hence, the output of Algorithm 3 does not represent the SVD of  $U_{\ell+1}$ . Therefore, it becomes essential to check whether  $W$  is empty. If  $W$  is not empty, we proceed to update the SVD for the vectors contained in  $W$ . For additional details, please refer to [30]; however, as it is not required for the integro-differential equation, we have excluded it here.



It is worth mentioning that even though the output of Algorithm 3 may not represent the SVD of  $U_{\ell+1}$ ,  $Q[\Sigma R \mid W]$  serves as an approximation of  $U_{\ell+1}$ . We will utilize this approximation in the next section, as it is crucial for the computation of the equation (1.1).

## 4 Incremental SVD method for the integro-differential equation

This section focuses on the application of the incremental SVD algorithm to the parabolic integro-differential equation (1.1). Our approach is to simultaneously solve the integro-differential equation and incrementally update the SVD of the solution. By doing so, we store the solutions at all time steps in the four matrices of the SVD. As a result, we are able to address the issue of data storage in solving the integro-differential equation (1.1).

Due to the errors that may arise during the data compression process and the potential alterations caused by singular value truncation to previous storage, it becomes necessary for us to modify the traditional scheme (2.2). Below, we provide a brief discussion of our approach.

- (1) Use the initial condition  $u_h^0$  to compute the numerical solution at time step 1, which follows the traditional approach. However, we use  $\hat{u}_h^1$  to denote the numerical solution for consistency. Once we obtain  $\hat{u}_h^1$ , we compress  $\{u_h^0, \hat{u}_h^1\}$  and denote the corresponding compressed data as  $\{\tilde{u}_h^{1,0}, \tilde{u}_h^{1,1}\}$ .
- (2) Use the compressed data  $\{\tilde{u}_h^{1,0}, \tilde{u}_h^{1,1}\}$  to compute the numerical solution at time step 2, denoted by  $\hat{u}_h^2$ . Once we obtain  $\hat{u}_h^2$ , we compress  $\{\tilde{u}_h^{1,0}, \tilde{u}_h^{1,1}\}$  and  $\hat{u}_h^2$ , and denote the corresponding compressed data as  $\{\tilde{u}_h^{2,0}, \tilde{u}_h^{2,1}, \tilde{u}_h^{2,2}\}$ .
- (3) At time step  $i$ , given the compressed data  $\{\tilde{u}_h^{i,j}\}_{j=0}^i$ , we compute the numerical solution at time step  $i+1$ , denoted by  $\hat{u}_h^{i+1}$ . We then compress  $\{\tilde{u}_h^{i,j}\}_{j=0}^i$  and  $\hat{u}_h^{i+1}$ , and denote the corresponding compressed data as  $\{\tilde{u}_h^{i+1,j}\}_{j=0}^{i+1}$ .
- (4) Continue the above process until we reach the final time step.

In summary, we apply our novel approach by incrementally compressing data at each time step to compute the numerical solutions throughout the process.

Based on the preceding discussion, we can present our formulation below, where we seek  $\hat{u}_h^{i+1} \in V_h$  that satisfies the following equation:

$$\left( \frac{\hat{u}_h^{i+1} - \hat{u}_h^i}{\Delta t}, v_h \right) + \mathcal{A}(\hat{u}_h^{i+1}, v_h) + \sum_{j=0}^i \omega_{i+1,j} \mathcal{B}(\tilde{u}_h^{i,j}, v_h) = (f^{i+1}, v_h) \quad \forall v_h \in V_h. \quad (4.1)$$

Subsequently, we express equation (4.1) into matrix form to highlight the benefits of utilizing the incremental SVD for solving the integro-differential equation more distinctly. To do this, let  $\hat{u}_{i+1}$  and  $\tilde{u}_{i,j}$  denote the coefficient of  $\hat{u}_h^{i+1}$  and  $\tilde{u}_h^{i,j}$ , respectively. Then we seek a solution  $\hat{u}_{i+1} \in \mathbb{R}^m$  that satisfies the following equation:

$$(M + \Delta t A) \hat{u}_{i+1} = M \hat{u}_i - \Delta t B \sum_{j=0}^i \omega_{i+1,j} \tilde{u}_{i,j} + \Delta t b_{i+1}. \quad (4.2)$$

Here,  $\{\tilde{u}_{i,j}\}_{j=0}^i$  represents the data that has been compressed from  $\{\tilde{u}_{i-1,0}, \dots, \tilde{u}_{i-1,i-1}, \hat{u}_i\}$  using the incremental SVD algorithm. We assume that  $Q_i$ ,  $\Sigma_i$ ,  $R_i$ , and  $W_i$  are the matrices associated with this compression process. In other words,

$$[\tilde{u}_{i-1,0} \mid \dots \mid \tilde{u}_{i-1,i-1} \mid \hat{u}_i] \xrightarrow{\text{Compress}} Q_i[\Sigma_i R_i \mid W_i]^\top = [\tilde{u}_{i,0} \mid \dots \mid \tilde{u}_{i,i}]. \quad (4.3)$$

Let  $[\Sigma_i R_i \mid W_i]^\top$  be denoted as  $X_i$ . Accordingly, equation (4.2) can be rewritten as follows:

$$(M + \Delta t A)\hat{u}_{i+1} = M\hat{u}_i - \Delta t B Q_i \sum_{j=0}^i \omega_{i+1,j} X_i(:, j) + \Delta t b_i. \quad (4.4)$$

Once  $\hat{u}_{i+1}$  is obtained, we update the SVD of  $[\tilde{u}_{i,0} \mid \dots \mid \tilde{u}_{i,i} \mid \hat{u}_{i+1}]$  using  $Q_i$ ,  $\Sigma_i$ ,  $R_i$ ,  $W_i$ , and  $\hat{u}_{i+1}$  based on the principles of the incremental SVD method. This update process is illustrated in Figure 1.

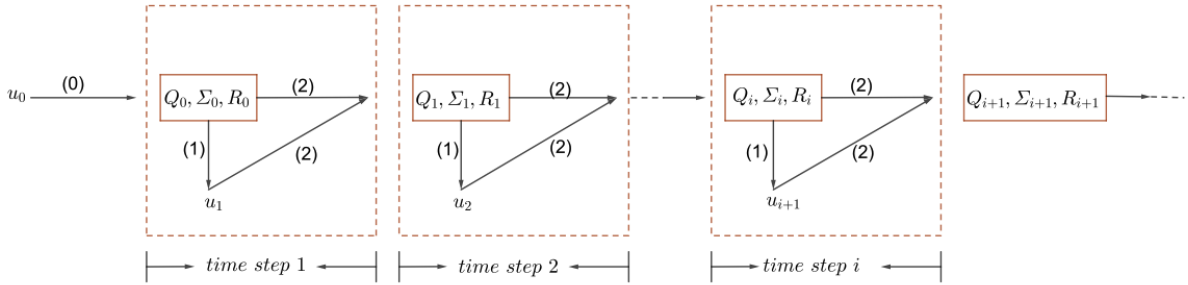


Figure 1: The process of using the incremental SVD to solve the integro-differential equation.

Throughout the remainder of this section, we will examine the memory and computational cost pertaining to the history term in our novel approach. Our data storage involves four matrices:  $Q_i$ ,  $\Sigma_i$ ,  $R_i$ , and  $W_i$ , resulting in a memory cost of  $\mathcal{O}((m+n)r)$ , where  $r$  represents the rank of the solution data. By taking into account our assumption that  $r \ll \min\{m, n\}$ , we can compare this memory cost with that of the traditional approach presented in (2.7), which illuminates a noteworthy reduction in our innovative method.

Moving on to the computational cost, which also encompasses the cost of the incremental SVD, it can be summarized as follows:

$$\mathcal{O}(mnr) + \sum_{i=1}^n \sum_{j=0}^i \mathcal{O}(r) = \mathcal{O}(mnr + rn^2).$$

Here, once again,  $r$  represents the rank of the solution data. Based on our assumption that  $r \ll \min\{m, n\}$ , we can compare the computational cost in (2.8) to that of the traditional approach, revealing that our approach experiences only linear growth, rather than quadratic growth as observed in the traditional approach.

## 5 Error estimate

In this section, we derive the error between the solution of the scheme (4.1) and the exact solution that satisfies the equation (1.1).

---

**Algorithm 4** (Incremental SVD for integro-differential equation)
 

---

**Require:**  $\Delta t, n, M \in \mathbb{R}^{m \times m}, A \in \mathbb{R}^{m \times m}, u_0, \text{tol}$ 

```

1: Set  $W = []$ ;  $Q_0 = 1$ ;  $\tilde{A} = M + \Delta t A$ ;  $\hat{u} = u_0$ ;
2:  $[Q, \Sigma, R] = \text{InitializeISVD}(u_0)$ ; Algorithm 2
3: for  $i = 0, 1, \dots, n-1$  do
4:   Compute the coefficients  $\omega_{i+1,j}$ ,  $j = 0, 1, \dots, i$ , and get the load vector  $b_{i+1}$ ;
5:   if  $W$  is empty then
6:      $\mathbf{M}Q = MQ$ ;  $X = \Sigma R^\top$ ;  $\mathbf{B}Q = BQ$ ;
7:      $\tilde{b}_{i+1} = M\hat{u} - \Delta t \mathbf{B}Q \sum_{j=0}^i \omega_{i+1,j} X(:, j+1) + \Delta t b_{i+1}$ ;
8:     Solve  $\tilde{A}\hat{u} = \tilde{b}_{i+1}$ ;
9:      $[Q, \Sigma, R, W, Q_0, q] = \text{UpdateISVD}(Q, \Sigma, R, \text{tol}, W, Q_0, q, \hat{u})$ ; Algorithm 3
10:    if  $W$  is not empty then
11:       $X = \Sigma R^\top$ ;
12:    end if
13:  else
14:     $D = [X \quad \text{cell2mat}(W)]$ ;
15:     $\tilde{b}_{i+1} = Mv - \Delta t \sum_{j=0}^i \omega_{i+1,j} \mathbf{B}QD(:, j+1) + \Delta t b_{i+1}$ ;
16:    Solve  $\tilde{A}\hat{u} = \tilde{b}_{i+1}$ ;
17:     $[Q, \Sigma, R, W, Q_0, q] = \text{UpdateISVD}(Q, \Sigma, R, \text{tol}, W, Q_0, q, \hat{u})$ ; Algorithm 3
18:  end if
19: end for
Ensure:  $\hat{u}$ 

```

---

### 5.1 Assumptions and Main Result

We assume throughout that  $\Omega$  is a bounded convex polyhedral domain, the data of (1.1) satisfies the following conditions:

(A1) Let  $\|\psi\|_a^2 = \mathcal{A}(\psi, \psi)$  for  $\psi \in H_0^1(\Omega)$ .  $\|\cdot\|_a$  is a norm and is equivalent to  $\|\cdot\|_1$  on  $H_0^1(\Omega)$ . There exists  $c_0 > 0$  such that

$$|\mathcal{B}(u, v)| \leq c_0 \lambda_0^{\beta/2-1} \|u\|_a \|v\|_a, \quad \forall u, v \in H_0^1(\Omega),$$

where  $\beta$  is the order of the operator  $B$ , and  $\lambda_0 = \lambda_0(\Omega, \mathcal{A}) > 0$  is the first eigenvalue of the elliptic problem

$$\mathcal{A}\phi - \lambda\phi = 0, \quad x \in \Omega \quad \text{and} \quad \phi = 0, \quad x \in \partial\Omega.$$

(A2) Let  $K_0 = \int_0^T K(t)dt$ , the following inequality holds:

$$c_0 K_0 \lambda_0^{\beta/2-1} < 1.$$

(A3) Let  $\mu = \max\{\mu_0\}$ , where  $\mu_0$  are the solutions of

$$1 - c_0 K_{\mu_0} \lambda_0^{\beta/2-1} \geq \frac{\mu_0}{\lambda_0}, \quad 0 < \mu_0 < \lambda_0,$$

where  $K_{\mu_0} = \int_0^T e^{\mu_0 t} K(t)dt$ .

(A4) Let

$$K_\mu^{\Delta t} = \max_{1 \leq i \leq n} \sum_{j=0}^i \omega_{i+1,j} e^{\mu(t_i - t_j)}$$

for any  $0 < \mu_0$  small, there exists a small  $T_0 > 0$  such that  $0 < \Delta t \leq T_0$ ,

$$1 - c_0 \lambda_0^{\beta/2-1} K_{\mu_0}^{\Delta t} e^{\mu_0 \Delta t} \geq \frac{\mu_0}{\lambda_0} e^{\mu_0 \Delta t}.$$

**Remark 3.** It is worth noting that conditions (A1)-(A3) are imposed to ensure the dominance of the operator  $\mathcal{A}$  over the integral term. The presence of  $\mu > 0$  in (A3) is a consequence of (A2). These same assumptions were employed in the work of [1] to establish the stability of the standard finite element method.

Now, we state the main result of our paper.

**Theorem 1.** Let  $u$  and  $\widehat{u}_h^n$  denote the solution of (1.1) and (4.1), respectively. Throughout the entire process of the incremental SVD algorithm, the tolerance  $\mathbf{tol}$  is applied to both  $p$ -truncation and singular value truncation. Under assumptions (A1) - (A4), if  $u(t) \in H^{k+1}(\Omega)$ , then the following error bound holds:

$$\|u(t_n) - \widehat{u}_h^n\| \leq C(h^{k+1} + \Delta t) + (T_{sv} + 1)\sqrt{T(1 + \gamma^{-1})\sigma(A)}\mathbf{tol}, \quad (5.1)$$

where  $C$  and  $\gamma \in (0, 2c_0^{-1}K_0^{-1}\lambda_0^{1-\beta/2} - 2)$  are two positive constants, independent of  $h$ ,  $\Delta t$ , and  $\mathbf{tol}$ , and  $\sigma(A)$  represents the spectral radius of the stiffness matrix  $A$ ,  $T_{sv}$  signifies the total number of times singular value truncation is applied.

## 5.2 Proof of Theorem 1

We begin by giving an error bound between the solution of the standard finite element method given by equation (2.3) and the solution of the Non-Fickian model (1.1). Additionally, we derive an error bound between the solution of the standard finite element method (2.3) and our novel scheme (4.1). By applying the triangle inequality, we obtain a straightforward error bound between the solution of the Non-Fickian model (1.1) and our novel scheme (4.1).

**Lemma 3.** [1, Theorem 4.4] Let  $u$  and  $u_h^n$  be the solution of (1.1) and (2.3) respectively. Assume that the conditions (A1)-(A4) hold and  $\|u_0 - u_h^0\| \leq Ch^{k+1} \|u_0\|_{k+1}$ . Then there exists a constant  $C > 0$ , independent of  $h$  and  $\Delta t$ , such that

$$\|u(t_n) - u_h^n\| \leq C(h^{k+1} + \Delta t). \quad (5.2)$$

Now, we will proceed to establish the error estimation between the solution of the standard finite element method (2.3) and our novel scheme (4.1).

**Lemma 4.** Let  $u_h^n$  and  $\widehat{u}_h^n$  be the solution of (2.3) and (4.1), respectively. Given assumptions (A1) and (A2), the following error bound is established:

$$\|u_h^n - \widehat{u}_h^n\| \leq \sqrt{T(1 + \gamma^{-1})} \max_{0 \leq i \leq n-1} \max_{0 \leq j \leq i} \|\widetilde{u}_h^{i,j} - \widehat{u}_h^j\|_a,$$

where  $\gamma \in (0, 2c_0^{-1}K_0^{-1}\lambda_0^{1-\beta/2} - 2)$  and  $c_0, \lambda_0, K_0$  are defined in assumptions (A1)-(A2).

*Proof.* Recall that  $u_h^{i+1}$  and  $\widehat{u}_h^{i+1}$  satisfy the following equations

$$\left( \frac{u_h^{i+1} - u_h^i}{\Delta t}, v_h \right) + \mathcal{A}(u_h^{i+1}, v_h) + \sum_{j=0}^i \omega_{i+1,j} \mathcal{B}(u_h^j, v_h) = (f^{i+1}, v_h), \quad \forall v_h \in V_h, \quad (5.3a)$$

$$\left( \frac{\widehat{u}_h^{i+1} - \widehat{u}_h^i}{\Delta t}, v_h \right) + \mathcal{A}(\widehat{u}_h^{i+1}, v_h) + \sum_{j=0}^i \omega_{i+1,j} \mathcal{B}(\widehat{u}_h^j, v_h) = (f^{i+1}, v_h), \quad \forall v_h \in V_h. \quad (5.3b)$$

Subtracting (5.3a) from (5.3b) and introducing two notations:  $\widehat{e}_{i+1} = u_h^{i+1} - \widehat{u}_h^{i+1}$ , and  $\widetilde{e}_{i,j} = u_h^j - \widehat{u}_h^j$ ,  $j = 0, 1, \dots, i$ , we obtain the following equation:

$$\left( \frac{\widehat{e}_{i+1} - \widehat{e}_i}{\Delta t}, v_h \right) + \mathcal{A}(\widehat{e}_{i+1}, v_h) + \sum_{j=0}^i \omega_{i+1,j} \mathcal{B}(\widetilde{e}_{i,j}, v_h) = 0, \quad \forall v_h \in V_h. \quad (5.4)$$

Substituting  $v_h = \widehat{e}_{i+1} \in V_h$  into the above equation and utilizing the identity  $2(a - b, a) = \|a\|^2 - \|b\|^2 + \|a - b\|^2$ , we derive the following equation:

$$(2\Delta t)^{-1} \left( \|\widehat{e}_{i+1}\|^2 - \|\widehat{e}_i\|^2 + \|\widehat{e}_{i+1} - \widehat{e}_i\|^2 \right) + \|\widehat{e}_{i+1}\|_a^2 = - \sum_{j=0}^i \omega_{i+1,j} \mathcal{B}(\widetilde{e}_{i,j}, \widehat{e}_{i+1}).$$

Using Cauchy-Schwarz inequality, assumption (A1), we can deduce the following equation:

$$\begin{aligned} & (2\Delta t)^{-1} \left( \|\widehat{e}_{i+1}\|^2 - \|\widehat{e}_i\|^2 + \|\widehat{e}_{i+1} - \widehat{e}_i\|^2 \right) + \|\widehat{e}_{i+1}\|_a^2 \\ & \leq \sum_{j=0}^i c_0 \lambda_0^{\beta/2-1} \omega_{i+1,j} \|\widetilde{e}_{i,j}\|_a \|\widehat{e}_{i+1}\|_a \\ & \leq \frac{c_0 \lambda_0^{\beta/2-1}}{2} \sum_{j=0}^i \omega_{i+1,j} \|\widetilde{e}_{i,j}\|_a^2 + \frac{c_0 \lambda_0^{\beta/2-1}}{2} \sum_{j=0}^i \omega_{i+1,j} \|\widehat{e}_{i+1}\|_a^2 \\ & \leq \frac{c_0 \lambda_0^{\beta/2-1}}{2} \sum_{j=0}^i \omega_{i+1,j} (\|\widetilde{e}_{i,j} - \widehat{e}_j\|_a + \|\widehat{e}_j\|_a)^2 + \frac{c_0 \lambda_0^{\beta/2-1}}{2} \sum_{j=0}^i \omega_{i+1,j} \|\widehat{e}_{i+1}\|_a^2 \\ & \leq \frac{c_0 \lambda_0^{\beta/2-1}}{2} \sum_{j=0}^i \omega_{i+1,j} ((1 + \gamma) \|\widehat{e}_j\|_a^2 + (1 + \gamma^{-1}) \|\widetilde{e}_{i,j} - \widehat{e}_j\|_a^2) + \frac{c_0 \lambda_0^{\beta/2-1}}{2} \sum_{j=0}^i \omega_{i+1,j} \|\widehat{e}_{i+1}\|_a^2 \end{aligned}$$

for some  $\gamma \in (0, 1)$ . Summing over  $i$  ranging from 0 to  $n - 1$ , we have:

$$\begin{aligned}
& (2\Delta t)^{-1} \left( \|\widehat{e}_n\|^2 - \|\widehat{e}_0\|^2 + \sum_{i=0}^{n-1} \|\widehat{e}_{i+1} - \widehat{e}_i\|^2 \right) + \sum_{i=0}^{n-1} \|\widehat{e}_{i+1}\|_a^2 \\
& \leq \frac{c_0 \lambda_0^{\beta/2-1}}{2} \sum_{i=0}^{n-1} \sum_{j=0}^i \omega_{i+1,j} ((1+\gamma) \|\widehat{e}_j\|_a^2 + (1+\gamma^{-1}) \|\widetilde{e}_{i,j} - \widehat{e}_j\|_a^2) \\
& \quad + \frac{c_0 \lambda_0^{\beta/2-1}}{2} \sum_{i=0}^{n-1} \sum_{j=0}^i \omega_{i+1,j} \|\widehat{e}_{i+1}\|_a^2 \\
& \leq \frac{c_0 \lambda_0^{\beta/2-1} (1+\gamma)}{2} \sum_{i=0}^{n-1} \sum_{j=i}^{n-1} \omega_{j+1,i} \|\widehat{e}_i\|_a^2 + \frac{c_0 \lambda_0^{\beta/2-1} (1+\gamma^{-1})}{2} \sum_{i=0}^{n-1} \sum_{j=0}^i \omega_{i+1,j} \|\widetilde{e}_{i,j} - \widehat{e}_j\|_a^2 \\
& \quad + \frac{c_0 \lambda_0^{\beta/2-1}}{2} \sum_{i=0}^{n-1} \sum_{j=0}^i \omega_{i+1,j} \|\widehat{e}_{i+1}\|_a^2 \\
& \leq \frac{2+\gamma}{2} c_0 \lambda_0^{\beta/2-1} K_0 \sum_{i=0}^{n-1} \|\widehat{e}_{i+1}\|_a^2 + \frac{c_0 \lambda_0^{\beta/2-1} (1+\gamma^{-1})}{2} K_0 \sum_{i=0}^{n-1} \max_{0 \leq j \leq i} \|\widetilde{e}_{i,j} - \widehat{e}_j\|_a^2.
\end{aligned} \tag{5.5}$$

Using assumption (A2), we can choose  $\gamma \in (0, 2c_0^{-1} K_0^{-1} \lambda_0^{1-\beta/2} - 2)$  such that

$$\frac{2+\gamma}{2} c_0 \lambda_0^{\beta/2-1} K_0 < 1.$$

Then (5.5) becomes

$$\begin{aligned}
\|\widehat{e}_n\|^2 & \leq \|\widehat{e}_0\|^2 + c_0 K_0 \lambda_0^{\beta/2-1} (1+\gamma^{-1}) T \max_{0 \leq i \leq n-1} \max_{0 \leq j \leq i} \|\widetilde{e}_{i,j} - \widehat{e}_j\|_a^2 \\
& \leq (1+\gamma^{-1}) T \max_{0 \leq i \leq n-1} \max_{0 \leq j \leq i} \|\widetilde{e}_{i,j} - \widehat{e}_j\|_a^2.
\end{aligned}$$

The proof is finalized by utilizing  $\widehat{e}_0 = 0$  along with the condition  $c_0 K_0 \lambda_0^{\beta/2-1} < 1$  (Assumption A2).  $\square$

Next we turn to estimate the term  $\max_{0 \leq i \leq n-1} \max_{0 \leq j \leq i} \|\widetilde{u}_h^{i,j} - \widehat{u}_h^j\|_a$ . We have the following error bound:

**Lemma 5.** Let  $\{\widehat{u}_h^i\}_{i=1}^n$  be the solution of (2.3), and let  $\{\widetilde{u}_h^{i,j}\}_{j=0}^i$  represent the compressed data corresponding to  $\{\widetilde{u}_h^{i-1,0}, \widetilde{u}_h^{i-1,1}, \dots, \widetilde{u}_h^{i-1,i-1}, \widehat{u}_h^i\}$ . This compressed solution is obtained using the incremental SVD method with a tolerance of `tol` applied to both  $p$ -truncation and singular value truncation. Let  $T_{sv}$  represent the total number of times the singular value truncation is applied, then we can obtain the following inequality:

$$\max_{0 \leq i \leq n-1} \max_{0 \leq j \leq i} \|\widetilde{u}_h^{i,j} - \widehat{u}_h^j\|_a \leq (T_{sv} + 1) \sqrt{\sigma(A)} \text{tol},$$

where  $\sigma(A)$  represents the spectral radius of the stiffness matrix  $A$ .

*Proof.* Assuming  $\hat{u}_j$  and  $\tilde{u}_{k,\ell}$  are the coefficients of  $\hat{u}_h^j$  and  $\tilde{u}_h^{k,\ell}$  corresponding to the finite element basis functions  $\{\phi_s\}_{s=1}^m$ , respectively, we establish the following inequality for  $0 \leq j \leq i-1 \leq n-1$ :

$$\begin{aligned} \|\tilde{u}_h^{i,j} - \hat{u}_h^j\|_a &\leq \sum_{k=0}^{i-j-1} \|\tilde{u}_h^{i-k,j} - \tilde{u}_h^{i-k-1,j}\|_a + \|\tilde{u}_h^{j,j} - \hat{u}_h^j\|_a \\ &= \sum_{k=0}^{i-j-1} \sqrt{(\tilde{u}_{i-k,j} - \tilde{u}_{i-k-1,j})^\top A (\tilde{u}_{i-k,j} - \tilde{u}_{i-k-1,j})} + \sqrt{(\tilde{u}_{j,j} - \hat{u}_j)^\top A (\tilde{u}_{j,j} - \hat{u}_j)} \\ &\leq \sum_{k=0}^{i-j-1} \sqrt{\sigma(A)} |\tilde{u}_{i-k,j} - \tilde{u}_{i-k-1,j}| + \sqrt{\sigma(A)} |\tilde{u}_{j,j} - \hat{u}_j|. \end{aligned}$$

Here,  $\sigma(A)$  represents the spectral radius of the stiffness matrix  $A$ . It is notable that  $\tilde{u}_{i-k,j}$  corresponds to the  $j$ -th compressed data at the  $i-k$ -th step, as illustrated by:

$$[\tilde{u}_{i-k-1,0} \mid \tilde{u}_{i-k-1,1} \mid \dots \mid \tilde{u}_{i-k-1,i-k-2} \mid \hat{u}_{i-k-1}] \xrightarrow{\text{Compressed}} [\tilde{u}_{i-k,0} \mid \tilde{u}_{i-k,1} \mid \dots \mid \tilde{u}_{i-k,i-k}].$$

Furthermore, considering that both  $p$  truncation and no truncation maintain the prior data unchanged, it follows that at most  $\min\{T_{sv}, i-j-1\}$  terms of  $\{\tilde{u}_{i-k,j} - \tilde{u}_{i-k-1,j}\}_{k=0}^{i-j-1}$  are non-zero, where  $T_{sv}$  represents the total number of times singular value truncation is applied. Consequently, for any  $0 \leq j \leq i-1 \leq n-1$ , employing Lemma 2, we can derive:

$$\max_{0 \leq i \leq n-1} \max_{0 \leq j \leq i} \|\tilde{u}_h^{i,j} - \hat{u}_h^j\|_a \leq (T_{sv} + 1) \sqrt{\sigma(A)} \mathbf{tol}.$$

□

Hence, by applying the triangle inequality to Lemmas 3 to 5, we can derive the error estimate for  $\|u(t_n) - \hat{u}_h^n\|$ . This completes the proof of Theorem 1.

## 6 Numerical experiments

This section comprises several numerical experiments conducted to show the efficiency and accuracy of our scheme (4.1). In the following scenario, we consider a case where the exact solution is known for (1.1). Let  $\Omega = (0, 1) \times (0, 1)$ ,  $\mathcal{A}u = -\Delta u$ ,  $\mathcal{B}u = -\frac{1}{10}\Delta u$ ,  $K(t) = e^{-t}$ , and the exact solution is given as:

$$u(x, y, t) = xy(1-x)(1-y)e^{-t} \cos t.$$

We can compute the initial condition  $u_0$  and the source term  $f$  using the provided data.

We employ linear finite element for the spatial discretization and utilize the backward Euler method for the time discretization.

In the accuracy test, we set  $\mathbf{tol} = 10^{-12}$  and the final time  $T = 1$ . The convergence rates of  $\|u(t_n) - \hat{u}_h^n\|$  are reported in Section 6 for fixed time steps  $\Delta t = 10^{-3}$  and  $\Delta t = 10^{-4}$ , while varying the mesh size  $h$  to assess the convergence rates in space. Additionally, the convergence rates of  $\|u(t_n) - \hat{u}_h^n\|$  are reported in Section 6 for a fixed mesh size  $h = 2^{-9}\sqrt{2}$ , while varying the time step  $\Delta t$  to evaluate the convergence rates in time. This verifies the first two terms in our error estimation (5.1).

In order to validate the final error term in (5.1), we calculate the numerical solution utilizing the finite element method and document the discrepancy between the outcomes of the conventional

finite element method (2.3) and our innovative approach (4.1) in Section 6. It is noteworthy that the errors align closely with machine precision, confirming the correspondence with the last element in our error estimation (5.1).

Additionally, we compare the wall time and memory for both the finite element method and our approach and plot four figures for intuition. It is evident that our new approach is more efficient, especially when the time step and mesh size are small. This suggests that our scheme performs well for large-scale problems.

$\Delta t$	$h/\sqrt{2}$	$\ u(t_n) - \hat{u}_h^n\ $	rate	$\Delta t$	$h/\sqrt{2}$	$\ u(t_n) - \hat{u}_h^n\ $	rate
$10^{-3}$	$1/2^2$	1.20E-03	-	$10^{-4}$	$1/2^2$	1.20E-03	-
	$1/2^3$	3.15E-04	1.93		$1/2^3$	3.15E-04	1.93
	$1/2^4$	8.01E-05	1.98		$1/2^4$	8.03E-05	1.97
	$1/2^5$	2.00E-05	2.00		$1/2^5$	2.01E-05	1.99
	$1/2^6$	4.84E-06	2.05		$1/2^6$	5.03E-06	2.00
	$1/2^7$	1.05E-06	2.20		$1/2^7$	1.24E-06	2.03

Table 1: The convergence rates of  $\|u(t_n) - \hat{u}_h^n\|$  for  $\Delta t = 10^{-3}$  and  $\Delta t = 10^{-4}$  with different mesh size  $h$ .

$h/\sqrt{2}$	$\Delta t$	$\ \hat{u}_h^n - u(t_n)\ $	rate	$h/\sqrt{2}$	$\Delta t$	$\ \hat{u}_h^n - u(t_n)\ $	rate
$1/2^9$	$1/2^2$	6.81E-05	—	$1/2^{10}$	$1/2^2$	6.81E-05	—
	$1/2^3$	3.24E-05	1.07		$1/2^3$	3.25E-05	1.07
	$1/2^4$	1.57E-05	1.05		$1/2^4$	1.58E-05	1.04
	$1/2^5$	7.68E-06	1.03		$1/2^5$	7.74E-06	1.03
	$1/2^6$	3.77E-06	1.03		$1/2^6$	3.83E-06	1.02
	$1/2^7$	1.84E-06	1.03		$1/2^7$	1.90E-06	1.01

Table 2: The convergence rates of  $\|u(t_n) - \hat{u}_h^n\|$  for  $h = 2^{-9}\sqrt{2}$  and  $h = 2^{-10}\sqrt{2}$  with different time step  $\Delta t$ .

$h/\sqrt{2}$	$\ u_h^n - \hat{u}_h^n\ $		
	$\Delta t = 10^{-2}$	$\Delta t = 10^{-3}$	$\Delta t = 10^{-4}$
$1/2^6$	1.50E-14	1.45E-14	3.14E-14
$1/2^7$	9.35E-15	1.10E-14	7.50E-14
$1/2^8$	1.26E-14	1.10E-14	3.21E-14
$1/2^9$	3.32E-14	8.81E-15	—

Table 3: — denotes that conventional finite element method cannot be accommodated due to memory constraints.



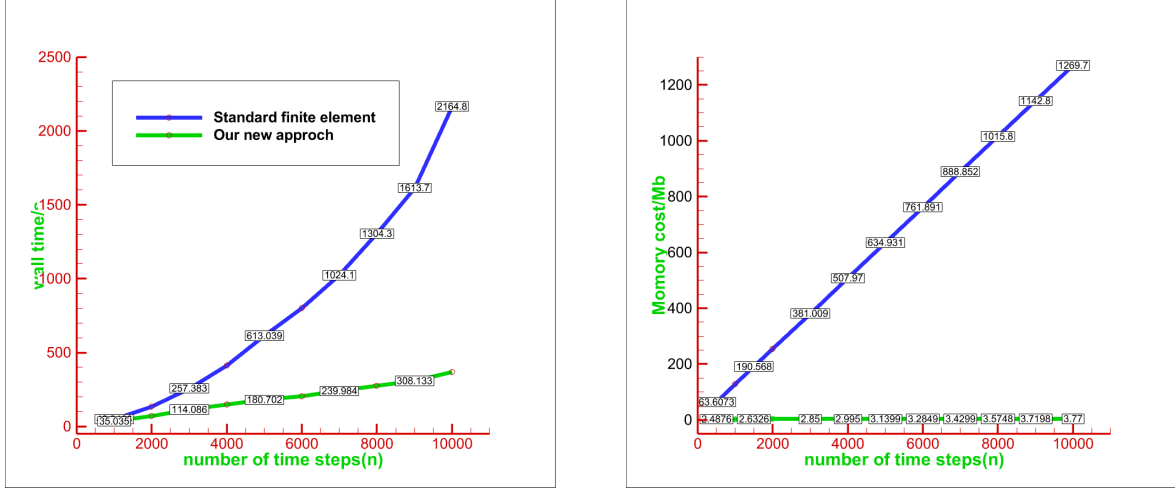


Figure 2: A comparison of wall time and memory costs between the two algorithms is conducted for various time steps, specifically when  $h = \sqrt{2}/2^7$  and  $\Delta t = 10^{-4}$ .

## 7 Conclusion

In this paper, we present a novel and efficient algorithm for resolving Non-Fickian flows. Our method draws inspiration from the incremental Singular Value Decomposition (SVD) technique commonly employed in data science. Notably, this approach exclusively operates on data intrinsic to the problem at hand. This adaptability leads us to posit its suitability for a range of significant models that encompass a memory component. A couple of such models include the Debye memory-enhanced Maxwell's equations [24]. These promising avenues form the focus of our upcoming research endeavors.

## References

- [1] W. ALLEGRETTO, Y. LIN, AND A. ZHOU, *Long-time stability of finite element approximations for parabolic equations with memory*, Numer. Methods Partial Differential Equations, 15 (1999), pp. 333–354.
- [2] S. BARBEIRO, S. G. BARDEJI, J. A. FERREIRA, AND L. PINTO, *Non-Fickian convection-diffusion models in porous media*, Numer. Math., 138 (2018), pp. 869–904.
- [3] N. BAUERMEISTER AND S. SHAW, *Finite-element approximation of non-Fickian polymer diffusion*, IMA J. Numer. Anal., 30 (2010), pp. 702–730.
- [4] M. BRAND, *Incremental singular value decomposition of uncertain data with missing values*, in Computer Vision—ECCV 2002: 7th European Conference on Computer Vision Copenhagen, Denmark, May 28–31, 2002 Proceedings, Part I 7, Springer, 2002, pp. 707–720.
- [5] —, *Fast low-rank modifications of the thin singular value decomposition*, Linear Algebra Appl., 415 (2006), pp. 20–30.
- [6] R. E. EWING, Y. LIN, T. SUN, J. WANG, AND S. ZHANG, *Sharp  $L^2$ -error estimates and superconvergence of mixed finite element methods for non-Fickian flows in porous media*, SIAM J. Numer. Anal., 40 (2002), pp. 1538–1560.

- [7] H. FAREED AND J. R. SINGLER, *Error analysis of an incremental proper orthogonal decomposition algorithm for PDE simulation data*, J. Comput. Appl. Math., 368 (2020), pp. 112525, 14.
- [8] H. FAREED, J. R. SINGLER, Y. ZHANG, AND J. SHEN, *Incremental proper orthogonal decomposition for PDE simulation data*, Comput. Math. Appl., 75 (2018), pp. 1942–1960.
- [9] J. A. FERREIRA AND L. PINTO, *An integro-differential model for non-Fickian tracer transport in porous media: validation and numerical simulation*, Math. Methods Appl. Sci., 39 (2016), pp. 4736–4749.
- [10] E. FROLOV AND I. OSELEDETS, *Tensor methods and recommender systems*, Wiley Interdisciplinary Reviews: Data Mining and Knowledge Discovery, 7 (2017), p. e1201.
- [11] L. GIRAUD, J. LANGOU, AND M. ROZLOZNIK, *The loss of orthogonality in the Gram-Schmidt orthogonalization process*, Comput. Math. Appl., 50 (2005), pp. 1069–1075.
- [12] M. S. HEMATI, M. O. WILLIAMS, AND C. W. ROWLEY, *Dynamic mode decomposition for large and streaming datasets*, Physics of Fluids, 26 (2014).
- [13] S. JIA, D. LI, AND S. ZHANG, *Asymptotic expansions and Richardson extrapolation of approximate solutions for integro-differential equations by mixed finite element methods*, Adv. Comput. Math., 29 (2008), pp. 337–356.
- [14] Z. JIANG,  *$L^\infty(L^2)$  and  $L^\infty(L^\infty)$  error estimates for mixed methods for integro-differential equations of parabolic type*, M2AN Math. Model. Numer. Anal., 33 (1999), pp. 531–546.
- [15] J. C. LÓPEZ MARCOS, *A difference scheme for a nonlinear partial integrodifferential equation*, SIAM J. Numer. Anal., 27 (1990), pp. 20–31.
- [16] G. MURALI MOHAN REDDY AND R. K. SINHA, *Ritz-Volterra reconstructions and a posteriori error analysis of finite element method for parabolic integro-differential equations*, IMA J. Numer. Anal., 35 (2015), pp. 341–371.
- [17] K. MUSTAPHA AND H. MUSTAPHA, *A second-order accurate numerical method for a semilinear integro-differential equation with a weakly singular kernel*, IMA J. Numer. Anal., 30 (2010), pp. 555–578.
- [18] G. M. OXBERRY, T. KOSTOVA-VASSILEVSKA, W. ARRIGHI, AND K. CHAND, *Limited-memory adaptive snapshot selection for proper orthogonal decomposition*, Internat. J. Numer. Methods Engrg., 109 (2017), pp. 198–217.
- [19] A. K. PANI AND G. FAIRWEATHER,  *$H^1$ -Galerkin mixed finite element methods for parabolic partial integro-differential equations*, IMA J. Numer. Anal., 22 (2002), pp. 231–252.
- [20] A. K. PANI, G. FAIRWEATHER, AND R. I. FERNANDES, *ADI orthogonal spline collocation methods for parabolic partial integro-differential equations*, IMA J. Numer. Anal., 30 (2010), pp. 248–276.
- [21] A. K. PANI AND T. E. PETERSON, *Finite element methods with numerical quadrature for parabolic integrodifferential equations*, SIAM J. Numer. Anal., 33 (1996), pp. 1084–1105.

- [22] B. RIVIÈRE AND S. SHAW, *Discontinuous Galerkin finite element approximation of nonlinear non-Fickian diffusion in viscoelastic polymers*, SIAM J. Numer. Anal., 44 (2006), pp. 2650–2670.
- [23] D. A. ROSS, J. LIM, R.-S. LIN, AND M.-H. YANG, *Incremental learning for robust visual tracking*, International journal of computer vision, 77 (2008), pp. 125–141.
- [24] S. SHAW, *Finite element approximation of Maxwell’s equations with Debye memory*, Adv. Numer. Anal., (2010), pp. Art. ID 923832, 28.
- [25] R. K. SINHA, R. E. EWING, AND R. D. LAZAROV, *Some new error estimates of a semidiscrete finite volume element method for a parabolic integro-differential equation with nonsmooth initial data*, SIAM J. Numer. Anal., 43 (2006), pp. 2320–2343.
- [26] ———, *Mixed finite element approximations of parabolic integro-differential equations with nonsmooth initial data*, SIAM J. Numer. Anal., 47 (2009), pp. 3269–3292.
- [27] I. H. SLOAN AND V. THOMÉE, *Time discretization of an integro-differential equation of parabolic type*, SIAM J. Numer. Anal., 23 (1986), pp. 1052–1061.
- [28] V. THOMÉE AND L. B. WAHLBIN, *Long-time numerical solution of a parabolic equation with memory*, Math. Comp., 62 (1994), pp. 477–496.
- [29] W. WANG AND Q. HONG, *Two-grid economical algorithms for parabolic integro-differential equations with nonlinear memory*, Appl. Numer. Math., 142 (2019), pp. 28–46.
- [30] Y. ZHANG, *An answer to an open question in the incremental SVD*, arXiv:2204.05398, (2022).